

# PPPM and TreePM Methods on GRAPE Systems for Cosmological N-body Simulations

Kohji YOSHIKAWA

*Department of Physics, School of Science,*

*University of Tokyo, Tokyo 133-0033*

*kohji@utap.phys.s.u-tokyo.ac.jp*

and

Toshiyuki FUKUSHIGE

*Department of General System Studies, College of Arts and Sciences,*

*University of Tokyo, Tokyo 153-8902*

*fukushig@providence.c.u-tokyo.ac.jp*

(Received ; accepted )

## Abstract

We present Particle–Particle–Particle–Mesh (PPPM) and Tree Particle–Mesh (TreePM) implementations on GRAPE-5 and GRAPE-6A systems, special-purpose hardware accelerators for gravitational many-body simulations. In our PPPM and TreePM implementations on GRAPE, the computational time is significantly reduced compared with the conventional implementations without GRAPE, especially under the strong particle clustering, and almost constant irrespective of the degree of particle clustering. We carry out the survey of two simulation parameters, the PM grid spacing and the opening parameter for the most optimal combination of force accuracy and computational speed. We also describe the parallelization of these implementations on a PC-GRAPE cluster, in which each node has one GRAPE board, and present the optimal configuration of simulation parameters for good parallel scalability.

**Key words:** methods: n-body simulations — cosmology: miscellaneous

## 1. Introduction

The Particle–Particle–Particle–Mesh (PPPM) method developed by Hockney & Eastwood (1981) has been recognized to be very versatile for studying particle systems in many branches of physics. In astrophysics, it has been widely used in a number of numerical simulations of cosmological structure formation (Efsthathiou et al. 1985; Bertschinger & Gelb 1991; Jing & Fang 1994; Jing & Suto 1998; Thomas & Couchman 1992; Yoshikawa et

al. 2000; Yoshikawa et al. 2001), since it was first applied to cosmological  $N$ -body simulation by Efstathiou & Eastwood (1981). This is because the PPPM method has several advantages that (1) it intrinsically satisfies the periodic boundary condition, (2) is faster under the light particle clustering, and (3) has a smaller memory requirement than other  $N$ -body algorithms such as the tree algorithm. The first one is important because, in cosmological  $N$ -body simulations, periodic boundary condition is required in order to perform realistic simulations of effectively “infinite” universe within a finite simulation volume.

Nowadays, however, the PPPM method in gravitational  $N$ -body simulations loses its attraction due to the fact that under the strong particle clustering, which is always realized through the gravitational instability as the system evolves, the cost of computing the gravitational forces is increased by a factor of ten, or even more, depending on the clustering strength and the number of particles adopted. In the PPPM method, the inter-particle force is split into two components: a long-range force calculated using the Particle–Mesh (PM) technique and a short-range one computed by directly summing up all the contribution from nearby particles within a given cutoff radius. The latter, Particle–Particle (PP) calculation, becomes unacceptably expensive under the strong particle clustering, while the computational cost of the PM calculation is independent of clustering degree of the particles.

In order to alleviate the drawback of the PPPM method described above while keeping its advantages, several modifications have been proposed. In the adaptive PPPM (AP3M) method developed by Couchman (1991), PP calculation is recursively split into further PM and PP calculation by setting up a refined mesh at regions where the particle clustering is strong. This method can significantly reduce the computational cost. However, even with the AP3M method, the calculation time increases as the particle clustering become strong by a factor of ten or so, depending on the number of particles and the degree of particle clustering. Another remedy for the PPPM method is to replace the PP calculation for short-range forces by the tree method, which is developed by Xu (1995), Bode, Ostriker, Xu (2000), Bagla (2002), and Bode & Ostriker (2003), and is called tree particle mesh (TreePM) method. This method reduces the expense of PP calculation under strong particle clustering, yet requiring additional memory.

The use of a special-purposed computer for gravitational  $N$ -body simulations, GRAPE (GRAvity PipE) system, provides us with a drastic reduction of computational load of the PP calculation in the PPPM method. For example, Brieu, Summers & Ostriker (1995) implement the PPPM method on GRAPE-3A system (Okumura et al. 1993) for cosmological  $N$ -body simulations. However, since the force shape of PP calculations in the PPPM method is different from the  $r^{-2}$  law, and GRAPE-3A can calculate only the  $r^{-2}$  gravitational force with softening, they had to approximate the force shape by combining three  $r^{-2}$  forces with different softening lengths and different weights. Due to this approximation, they found small but non-negligible systematic errors in clustering statistics in a cold dark matter simulation. Recently,

**Table 1.** GRAPE Summary

	# of chips	# of pipelines	Peak speed ( $10^9$ int/s)	Accuracy
GRAPE-5	8	16	1.28	$\sim 0.2\%$
GRAPE-6A	4	24	2.30	single precision

Susukita (2004) implemented the PPPM method on MDGRAPE-2 (Susukita et al. 2003), an extension of MD-GRAPE (Molecular Dynamics GRAPE) (Fukushige et al. 1996) which can compute forces with arbitrary shapes. The resulting performance of the PPPM implementation on MDGRAPE-2 system is  $\sim 10$  times better than that of AP3M implementation (Couchman 1991).

In this paper, we present the PPPM and TreePM implementations on GRAPE-5 (Kawai et al. 2000) and GRAPE-6A (Fukushige et al. 2005) systems, both of which have a capability to calculate the  $r^{-2}$  forces multiplied by a user-specified cutoff function, and have better performance than MDGRAPE-2. We also develop the parallelized versions of these implementations with Message Passing Interface (MPI) and estimate their scalability. As we show below, these implementations on GRAPE-5 and GRAPE-6A systems have sufficient advantage over those without GRAPE.

The outline of this paper is as follows. In § 2, the architectures of GRAPE-5 and GRAPE-6A are briefly described. § 3 is devoted to brief introduction of the PPPM and TreePM methods, their implementations on GRAPE-5 and GRAPE-6A, and their parallelization scheme. We evaluate the accuracy of force calculated using the PPPM and TreePM methods on GRAPE in § 4, and present their performance and memory requirement in § 5 and § 6, respectively. In § 7, we summarize our conclusion and give discussion on further improvement of our implementation on the future GRAPE systems.

## 2. GRAPE systems

GRAPE (Sugimoto et al. 1990; Makino & Taiji 1998) is a special-purpose computer to accelerate calculations of the gravitational interaction. GRAPE has pipelines specialized for the interaction calculations, which is the most expensive part of  $N$ -body simulations. The GRAPE hardware, connected to a standard PC or workstation (host computer), receives the positions and masses of particles and calculates the interactions between particles. All other calculations are performed on the host computer.

In Table 1, we summarize features of GRAPE-5 and GRAPE-6A that we used for implementations of the PPPM and TreePM methods in this paper. GRAPE-6A is a single PCI card with four GRAPE-6 processor chips (Makino et al. 2003), and is designed for PC-GRAPE cluster configuration (Fukushige et al. 2005). For details of GRAPE-5 and -6A, see Kawai et al. (2000), and Fukushige et al. (2005), respectively. The unit of the peak speed is  $10^9$  pair-wise

interactions per second. The GRAPE-5 system is currently no longer produced, but it is still available in several sites such as Astronomical Data Analysis Center in National Astronomical Observatory Japan <sup>1</sup>.

These GRAPEs calculate the gravitational force with an arbitrary cutoff function on particle  $i$ , given by equations:

$$\vec{f}_i = \sum_j \frac{m_j \vec{r}_{ij}}{r_{s,ij}^3} g(r_{s,ij}/\eta). \quad (1)$$

Here  $\vec{r}_j$  and  $m_j$  are the position and the mass of particle  $j$ ,  $\vec{r}_{ij} = \vec{r}_j - \vec{r}_i$ , and  $r_{s,ij}$  is the softened distance between particles defined as  $r_{s,ij}^2 \equiv r_{ij}^2 + \varepsilon^2$ , where  $\varepsilon$  is the softening length. The function  $g$  is an arbitrary cutoff function and  $\eta$  is the scaling length for the cutoff function. The cutoff function is necessary for the calculation of PP force in the PPPM and TreePM methods. The force is calculated with limited accuracy ( $\sim 0.2\%$  for pairwise) in GRAPE-5, and with single precision accuracy in GRAPE-6A. In the rest of this paper, we show the results only for GRAPE-6A system unless otherwise stated.

### 3. Algorithm and Implementation

In this section, we briefly describe the algorithms of PPPM and TreePM methods and their implementations on GRAPE systems. In addition, we also present our parallelization of these implementations using MPI.

#### 3.1. PPPM

The PPPM method is comprised of PM and PP parts which compute long and short-range components of inter-particle forces, respectively. In the PM part, the mass density on a regular grid (PM grid, hereafter) is computed by interpolating the particle positions, and the gravitational potential is calculated by solving the Poisson equation on this grid using Fast Fourier Transform (FFT). The force must be sufficiently smooth so that it can be well represented by the discrete grid. Therefore, it is assumed that each particle virtually have a spherical density profile which is usually denoted by  $S2$  profile (Eastwood, Hockney, & Lawrence 1980). In our implementation, we use the triangular-shaped cloud (TSC) scheme to calculate the mass density field on the PM grid, and the 4-point finite differential algorithm (FDA) to compute the particle accelerations by interpolating the gravitational potential field. The resulting gravitational force obeys the  $r^{-2}$  law beyond a softening length  $\varepsilon_{\text{PM}}$  (about two or three grid spacings), and is softened inside it. Usually, the required force shape has smaller softening length than the grid spacing. Therefore, we need an additional short-range component, which is non-zero only for particle pairs with separations smaller than  $\varepsilon_{\text{PM}}$ , to compute the total required force. In order to compensate for this short-range forces, the PP calculation accumulates the “residual” gravitational force, the required gravitational force minus that calculated in the PM

<sup>1</sup> [http://www.cc.nao.ac.jp/J/cc/muv/index\\_e.html](http://www.cc.nao.ac.jp/J/cc/muv/index_e.html)

part, contributed by all nearby particles lying within a certain cutoff radius  $r_{\text{cut}}$ . Specifically, for a given particle separation  $r$ , the force shape adopted in the PP part is given by

$$F_{\text{PP}}(r) = F_{\text{tot}}(r) - R(r, \varepsilon_{\text{PM}}), \quad (2)$$

where  $F_{\text{tot}}$  is the required total force,  $\varepsilon_{\text{PM}}$  the softening length for the PM force, and  $R(r, a)$  the force shape calculated in the PM part given by

$$R(r, a) = \begin{cases} (224\xi - 224\xi^3 + 70\xi^4 + 48\xi^5 - 21\xi^6)/35a^2 & 0 \leq \xi < 1 \\ (12/\xi^2 - 224 + 896\xi - 840\xi^2 + 224\xi^3 + 70\xi^4 - 48\xi^5 + 7\xi^6)/35a^2 & 1 \leq \xi < 2 \\ 1/r^2 & 2 \leq \xi, \end{cases} \quad (3)$$

where  $\xi = 2r/a$ . Note that  $R(r, a)$  follows  $r^{-2}$  law at  $r > a$ , and is softened at  $r < a$ . As described in section 2, GRAPEs calculate the Plummer-softened force. Therefore, the PPPM method on GRAPE systems naturally adopts the Plummer-softened force shape for  $F_{\text{tot}}(r)$  and

$$g_{\text{PP}}(r, \varepsilon_{\text{PM}}) = 1 - R(r, \varepsilon_{\text{PM}})/F_{\text{tot}}(r), \quad (4)$$

for the user-specified cutoff function  $g$  in equation (1). Since  $R(r, \varepsilon_{\text{PM}})$  deviates from  $r^{-2}$  at  $r < \varepsilon_{\text{PM}}$ , we set the cutoff radius to  $r_{\text{cut}} = \varepsilon_{\text{PM}}$ . Throughout in this paper, we set  $\varepsilon_{\text{PM}} = 3H$ , where  $H$  is the PM grid spacing. Figure 1 depicts the force shapes for the PM and PP calculations as well as the total force shape.

In the PP part, the simulation volume is divided into cubic chaining cells with a side equal to or greater than  $r_{\text{cut}}$ . For each chaining cell, a linked-list of particles is build to keep track of all the particles in that cell. With this linked-list, one can efficiently calculate the contribution on each particle in the cell from all nearby particles within the cutoff radius  $r_{\text{cut}}$ , by accumulating the pairwise interaction with all particles in that cell and in the adjacent 26 cells. In virtue of the symmetry of forces, we can eliminate the unnecessary double computations of force for each particle pair. In order to achieve this, the pairwise interactions are computed for all pairs of particles in the current chaining cell, and for all pairs with one particle in the current chaining cell and the other in one of 13 neighbor cells.

On GRAPE systems, however, the sum of all forces exerted on a particle is computed for a given set of interacting particles. Therefore, the benefit from symmetry of forces is not available and we have to implement the PP part in a different manner on GRAPE systems. The overall procedures to calculate PP force using GRAPE is as follows.

1. The host computer calculates the PM force.
2. The host computer constructs a linked-list of all particles.
3. Repeat 3.1 to 3.4 for all chaining cells
- 3.1. The host computer sends masses and positions of particles in current and 26 adjacent chaining cells to GRAPE as interacting particles.

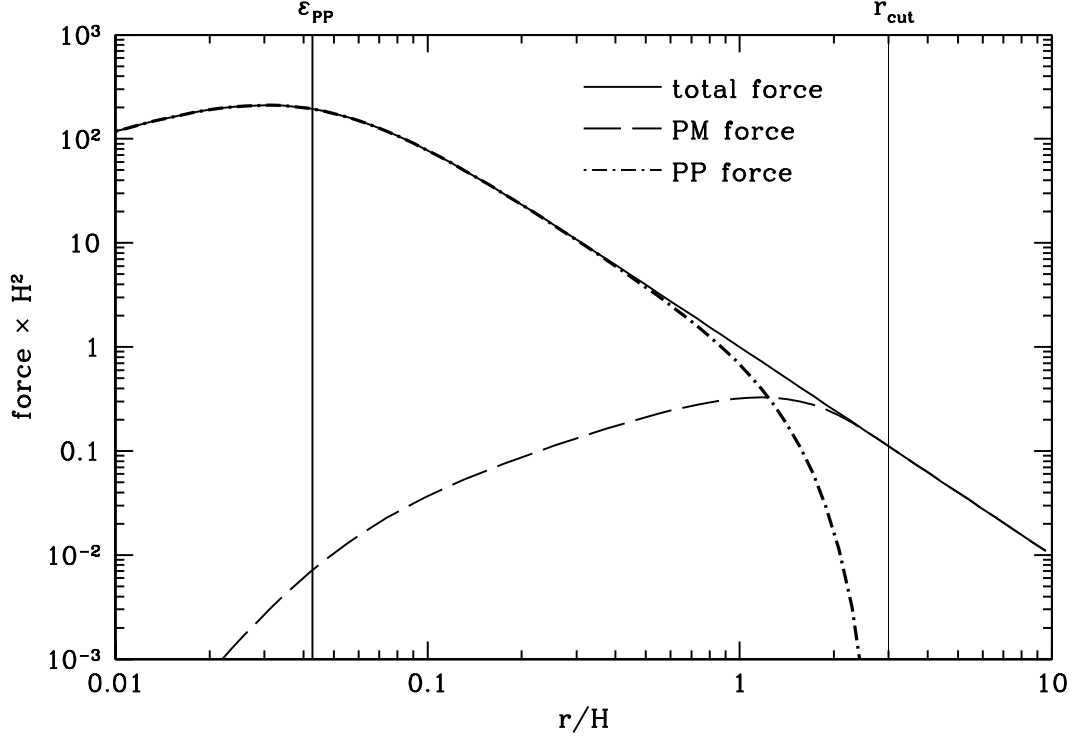


**Fig. 1.** Shapes of the total, PM and PP forces as a function of particle separation in units of the PM grid spacing. Vertical lines indicate the location of softening length  $\epsilon_{PP}$  and the cutoff radius  $r_{cut}$ .

- 3.2. The host computer sends positions of particles in the current chaining cell to GRAPE.
- 3.3. GRAPE calculates the PP forces exerted on the particles in the current chaining cell, which are sent to GRAPE in 3.2.
- 3.4. The PP forces computed by GRAPE in 3.3 are returned to the host computer.
4. The host computer augments the accelerations of particles in the current chaining cell using the calculated PP forces.
5. The host computer updates the positions and velocities of all particles using the calculated PM and PP forces.

On the GRAPE-5 chip, the particle index unit optimized for the linked-list method is equipped, with which we can reduce the communication cost between a host computer and GRAPE-5 (Kawai et al. 2000). In stead, on the GRAPE-6A system, since the particle index unit is not equipped, PP force calculation is done on a host computer (not on GRAPE-6A) if number of particles in the current chaining cell is less than a threshold  $n_{th}$  in order to reduce the communication overhead between a host computer and GRAPE-6A. In this paper, we set  $n_{th} = 10$ . Thus, the implementation of PP part for GRAPE-5 is slightly different from that for GRAPE-6A so as to make use of the particle index unit.

The spacing of PM grid controls the performance and memory requirement of the implementation. If we adopt larger spacing, we have larger cutoff radius and thus computational

cost for PP part increases. To the contrary, if smaller  $H$  is adopted, the cost for PM part increases and we need larger memory requirement. In the conventional PPPM implementation,  $H$  is usually set to  $\simeq L/(2N^{1/3})$ , where  $L$  is the size of simulation volume. In order to use GRAPE system efficiently, it is more advantageous to compute accelerations of as many particles as the number of (virtual) pipelines on GRAPE systems (96 for GRAPE-5 and 48 for GRAPE-6A) in the procedure 3.3 of the PP calculation listed above. In order to achieve this, in our implementation, the spacing of the PM grid  $H$  is set to

$$H = H_0 \equiv L/N^{1/3}, \quad (5)$$

which is two times larger than that usually adopted in the conventional PPPM implementation. Accordingly, we adopt larger  $\varepsilon_{\text{PM}}$  and  $r_{\text{cut}}$  since we set  $r_{\text{cut}} = \varepsilon_{\text{PM}}$  and  $\varepsilon_{\text{PM}} = 3H$ .

### 3.2. *TreePM*

TreePM is a method in which the direct calculation of PP force in the PPPM method is replaced by the hierarchical tree algorithm. In this section we briefly describe our implementation of the TreePM method on GRAPE.

Several studies on the Tree + PM hybrid implementations were already reported (Xu 1995; Bode, Ostriker, Xu 2000; Bagla 2002; Bode & Ostriker 2003; Dubinski et al. 2003), and they are divided into two categories. Xu (1995), Bode, Ostriker, Xu (2000) and Bode & Ostriker (2003) developed TPM in which tree algorithm is used for short range force only in dense cluster regions. Another is developed by Bagla (2002) and Dubinski et al. (2003), in which PP force is calculated with tree algorithm throughout the entire simulation volume. We implement the latter algorithm on GRAPE.

We modify a Barnes-Hut tree code (Barnes, & Hut 1986), which is originally used with vacuum boundary on GRAPE-5 (Fukushige & Suto 2001), so that (i) the functional form of gravitational force is  $1/r^2$  with a cutoff, expressed in equation (4), and (ii) the periodic boundary condition is taken into account in the tree traversal. We incorporated Barnes' modified algorithm (Barnes 1990) in order to make GRAPE work efficiently as described in Makino (1991). In the original algorithm, tree traversal is performed for each particle. In the modified algorithm, tree traversal is performed for a group of neighboring particles and an interaction list is created. GRAPE calculates the force from particles and the nodes in this interaction list to particles in the group.

The calculation procedure of the TreePM method on GRAPE is as follows:

1. The host computer calculates the PM force.
- 2.1. The host computer constructs a tree structure, and divide particles into groups of neighboring ones using the tree structure.
- 2.2. Repeat 2.3.-2.6. for all groups.
- 2.3. The host computer creates the interaction list for a group, and sends the data of the particles listed up to GRAPE.



- 2.4. Repeat 2.5.-2.6. for all particles in a group.
- 2.5. The host computer sends particles to be calculated to GRAPE.
- 2.6. GRAPE calculates the PP forces exerted on the particles, and then returns the result to the host computer.
3. The host computer updates the positions and velocities of all particles using the calculated PM and PP forces.

The modified tree algorithm reduces the calculation cost of the host computer by roughly a factor of  $n_g$ , where  $n_g$  is the average number of particle in groups. On the other hand, the amount of work on GRAPE increase as we increase  $n_g$ , since the interaction list becomes longer. There is, therefore, an optimal value of  $n_g$  at which the total computing time is minimum. The optimal value of  $n_g$  depends on various factor, such as the relative speed of GRAPE and its host computer, the opening parameter and the number of particles. For the present GRAPE-5 and -6A,  $n_g = 500 - 1000$  is close to optimal.

### 3.3. *Parallel PPPM and TreePM*

We also parallelize our PPPM and TreePM implementations using the one dimensional slice domain decomposition scheme and MPI library. Our parallel algorithm is similar to the parallel PPPM code by Brieu, & Evrard (2000) and GOTPM by Dubinski et al. (2003). The calculation procedure for the parallel PPPM and TreePM methods on GRAPE is as follows:

1. Particles are distributed into the slice domains, and each parallel node is responsible for particles in each slice domain. The boundaries of the slice domains are adjusted so that the number of particles in each domain is equal. As these boundaries move, particles are dynamically re-assigned to the parallel node responsible for the domain where they reside. Figure 2 is a schematic picture of the domain decomposition.
2. Each node calculates the mass density on the PM grid for the slice domain. The entire grid density are communicated and shared among all nodes. Then, each node calculates the gravitational potential on the PM grid using FFT, and compute the PM forces.
3. In the parallel PPPM, each node imports those particles from the neighboring domains which reside in its skirt regions with a width of  $r_{\text{cut}}$  from the domain boundaries. See Figure 2 for a schematic picture of the skirt regions. In each node, a linked-list is built for all the particles in the slice domain and the imported particles in the skirt regions. Then, the PP forces are calculated in the same manner as the serial PPPM implementation.

In the parallel TreePM, each node constructs a tree structure and makes the interaction list for the neighboring nodes. Each node receives the interaction lists from the neighboring nodes, and reconstruct the tree structure together with the received interaction lists. The PP forces for particles in the slice domain are calculated using the tree structure as done in the serial TreePM algorithm.



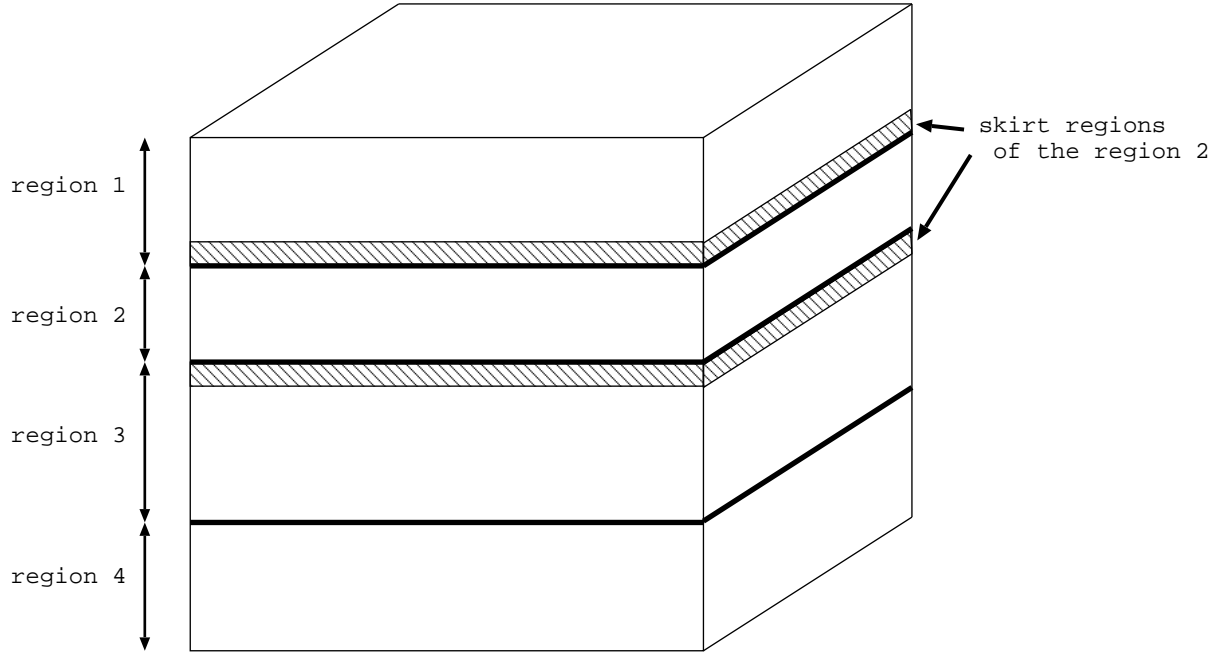


**Fig. 2.** Schematic picture of domain decomposition of simulation volume used in the parallel PPPM and TreePM calculations. Bold lines are the domain boundaries and shaded regions indicate the skirt regions of the region 2.

4. The positions and velocities of particles in each node are updated using the calculated PM and PP forces.
5. Those particles which get across the domain boundaries are exchanged between the neighboring nodes.

In these parallelization, the FFT is performed in a serial fashion, and the global potential field is computed independently by each node. Therefore, we have to communicate the density field on the PM grid among the nodes. As can be seen in Table 4 and 5, the CPU time required for these communication is not predominant, but cannot be neglected. Therefore, the use of parallel FFT may improve the overall parallel efficiency.

#### 4. Force Accuracy

Here, we discuss the force accuracy of the PPPM and TreePM methods on GRAPE. We calculated the forces using particle distributions from dark matter simulations in a spatially flat low density CDM (LCDM hereafter) cosmology with  $\Omega_m = 0.3$ ,  $\Omega_\Lambda = 0.7$ ,  $h = 0.7$ , and  $\sigma_8 = 0.9$  within a box size of  $L = 75h^{-1}$  Mpc, where  $\Omega_m$  is the density parameter,  $\Omega_\Lambda$  the dimensionless cosmological constants,  $h$  the Hubble parameter in units of  $100 \text{ km s}^{-1} \text{ Mpc}^{-1}$ , and  $\sigma_8$  the rms density fluctuation at a scale of  $8h^{-1}\text{Mpc}$ . In this section, we only show the results obtained using the GRAPE-6A board. The exact forces are computed using the direct Ewald summation (whose convergence parameters are set so that the relative force error is less than  $10^{-5}$ ). Here,

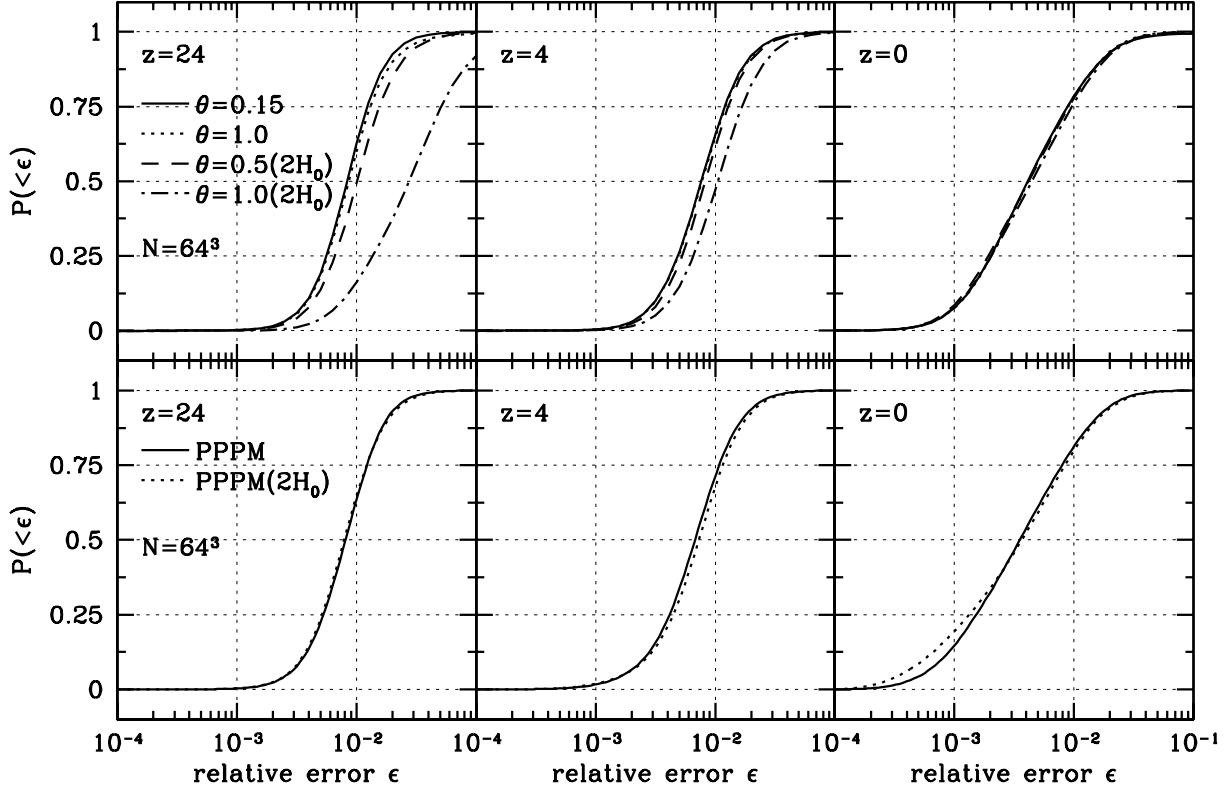


**Fig. 3.** The cumulative distribution of the relative error in the PPPM and TreePM methods on GRAPE for  $N = 64^3$ . Lines labeled as “ $2H_0$ ” indicate the error distribution for the PM grid spacing of twice the standard value.

we measured the relative force error given by

$$\epsilon_i = \frac{|\vec{f}_i - \vec{f}_{\text{ew},i}|}{|\vec{f}_i|}, \quad (6)$$

where  $\vec{f}_i$  and  $\vec{f}_{\text{ew},i}$  are force vectors of the  $i$ -th particle calculated using the PPPM or TreePM methods and the direct Ewald summation, respectively. Figure 3 and 4 show the cumulative distributions of the relative force error  $\epsilon$  in the PPPM (lower) and TreePM (upper) methods for the number of particles of  $N = 64^3$  and  $N = 128^3$ , respectively. For the TreePM method, we show the error distributions for various BH opening parameters,  $\theta$ .

As a matter of course, the force accuracy in the PPPM method is better than that of the TreePM method, since, in the latter, the direct sum calculation of PP part in the PPPM method is replaced by the tree method. The force accuracy and computational cost of the tree method is controlled by the opening parameter  $\theta$ . When the PM grid spacing are set to be the standard value,  $H = H_0$ , we can see in these figures that the error distributions in the TreePM method with  $\theta = 1.0$  and with  $\theta = 0.15$  are in good agreement with those in the PPPM method, independent of the number of particle,  $N$ , and the redshift  $z$  (i.e. clustering). This means that the error due to the tree force calculation when  $\theta \leq 1$  is small compared with the error in the

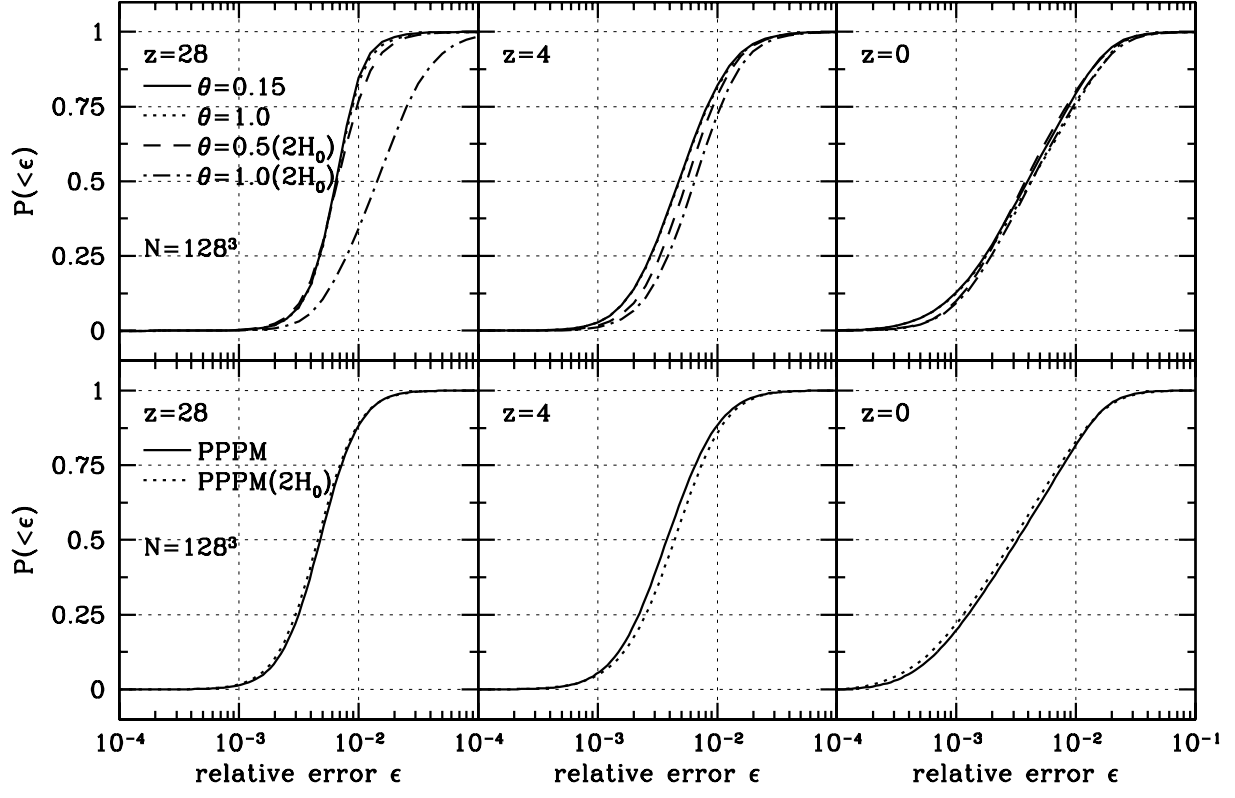


Fig. 4. Same as Figure 3, but for  $N = 128^3$ .

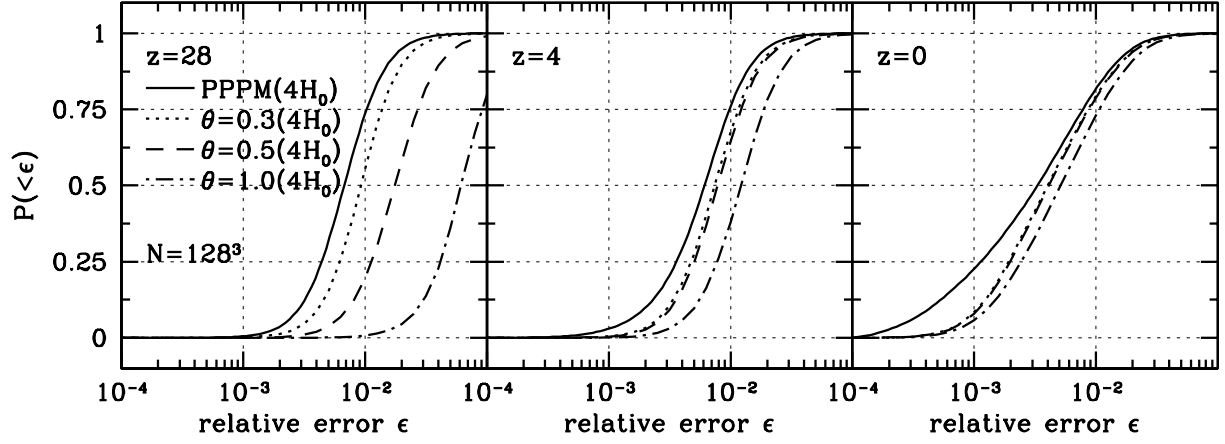


Fig. 5. Same as Figure 4, but for larger PM grid spacing,  $4H_0$ .

PM force calculation, which is nearly equivalent to the error distribution in the PPPM method. From these results, we conclude that in the TreePM method, the opening parameter,  $\theta = 1.0$ , is small enough when  $H = H_0$ . In general, the force accuracy in cosmological simulations using the tree algorithm is rather worse especially when the particle distribution is close to homogeneous. Since the tree method always needs to sum up the forces from all the particles or cells, and, under the homogeneous particle distribution, forces from individual particles or cells are much larger than the net forces, even if the relative errors of forces contributed from each particle or cell are small, the sum of large individual forces could result in large errors of the net force. However, in the case of TreePM, the force error is not so large as shown in Figure 3 and 4, simply because the long range force is computed using the PM method, and the contribution of the tree PP force is small.

We also check the force accuracy when the PM grid spacing are larger than the standard value,  $H_0$ . Using larger PM grid spacing, memory space for the PM calculations can be saved and a better scalability is expected for our present parallel implementation as will be discussed in the next section. In figure 3 and 4, the cumulative distributions of the relative force error for twice the standard value,  $2H_0$ , are also shown. In the PPPM method, the error distributions are almost unchanged compared with the case of the standard PM grid spacing. However, in the TreePM method, the force accuracy becomes worse when the particle distribution are close to homogeneous, since the contribution of PP calculation to the overall force computation is larger. At the beginning of simulations where the particle distribution is close to homogeneous, force calculation with  $\theta \leq 0.5$  is required. As the clustering proceeds the error due to tree algorithm becomes smaller, and  $\theta = 1.0$  is small enough at  $z \leq 4$ . Figure 5 shows the cumulative distribution for the PM grid spacing of  $4H_0$ . In this case, the force error becomes much worse in the TreePM method. The force calculations with  $\theta = 0.3, 0.5$  and  $1.0$  seem to be marginally acceptable at the initial epoch,  $z = 4$ , and  $z = 0$ , respectively. Also in the PPPM method, the force accuracy gets worse, but only slightly.

## 5. Performance

In this section, we present systematic measurements of the performance of the PPPM and TreePM implementations on GRAPE systems. We use dark matter simulations in LCDM cosmology within a box size of  $L = 75h^{-1}$  Mpc.

### 5.1. Serial Implementation

First, we discuss the performance for a single node configuration composed of one GRAPE-5/GRAPE-6A board and one host computer. In the following, the host computer for GRAPE-5 is equipped with Intel Pentium 4 (2.4GHz E7205) with 2GB of PC2001 memories, and that for GRAPE-6A has Intel Pentium 4 (2.8GHz, i865G) with 2GB of PC3200 memories. We use gcc compiler (version 3.2.2) on Redhat 9.0 (Linux kernel 2.4.20-8) through-

out in these measurement. We adopt the PM grid spacing of  $H = H_0$  in the simulations with GRAPE and  $H = H_0/2$  in those without GRAPE unless otherwise stated.

Figure 6 shows the CPU time per timestep as a function of redshift using the PPPM (lower) and TreePM (upper) methods for number of particles of  $N = 128^3$ . In both panels, we show the CPU time per timestep without GRAPE just for comparison. For the runs without GRAPE, the PPPM code is based on the implementation adopted in Jing & Suto (1998), and the TreePM code is modified so that the average number of particles in groups  $n_g$ , for which the tree traversal is performed, is reduced to  $n_g = 30$ . In the upper horizontal label, we show the ticks in the cosmic time normalized to a redshift of  $z = 0$ . In PPPM method without GRAPE, the CPU time at  $z = 0$  is  $\sim 13$  times longer than that at  $z = 28$ . This is well known drawback of the PPPM method under strong particle clustering at a lower redshift, which leads to the rapid increase of computational cost for PP calculation. For the PPPM method with the standard PM grid spacing  $H$ , although the CPU time with GRAPE-5 or GRAPE-6A at a higher redshift is 2–3 times longer than that without GRAPE, the use of GRAPE significantly reduces the CPU time at a lower redshift  $z < 1.5$  or  $t(z)/t(z=0) > 0.3$ , where  $t(z)$  is the cosmic time at a redshift of  $z$ . For the TreePM method with the standard PM grid spacing  $H_0$ , the CPU time on GRAPE is less than half of that for the PPPM method, if we adopt  $\theta > 0.5$ . In comparison with the TreePM method without GRAPE, when  $\theta = 1.0$  is adopted, we can obtain a speedup factor of 2.8 and 4.4 with GRAPE at redshift of  $z = 28$  and  $z = 0.0$ , respectively. This is in virtue of the tree algorithm used in the PP part instead of direct force calculation adopted in the PPPM method. The most remarkable feature of the PPPM and TreePM methods on GRAPE is that the CPU time per timestep is almost constant irrespective of redshift, or equivalently, the strength of particle clustering. In Figure 6, we also show the CPU time per timestep when we adopt larger PM grid spacing. Adopting larger PM grid spacing in the PPPM method increases the CPU time per timestep due to the increase of PP calculation. On the other hand, for the TreePM method, the CPU time is not much affected even if we adopt larger PM grid spacing. Figure 7 shows the CPU time per timestep plotted versus the opening parameters of tree algorithm for  $N = 64^3$  and  $128^3$ . For  $\theta > 0.7$ , the CPU time per timestep is almost constant, and for  $\theta \simeq 0.3$ , it is close to that of the PPPM method with the same number of particles.

Tables 2 and 3 give a breakdown of the calculation time for one timestep in the PPPM method and TreePM method, respectively. In these tables, "others", "tree", and "comm" indicate the time for mesh assignment and calculation of potentials and forces in the PM calculation, the time for tree construction and traversal, and the time for data communication between host computer and GRAPE and data conversion on host computer, respectively. Times labeled as "GRAPE" indicate those consumed by GRAPE chip, which is estimated by the number of interactions calculated by GRAPE chip. Specifically, these times are estimated using following formula:

$$T = (N_{\text{int}} + 100N)/P, \quad (7)$$

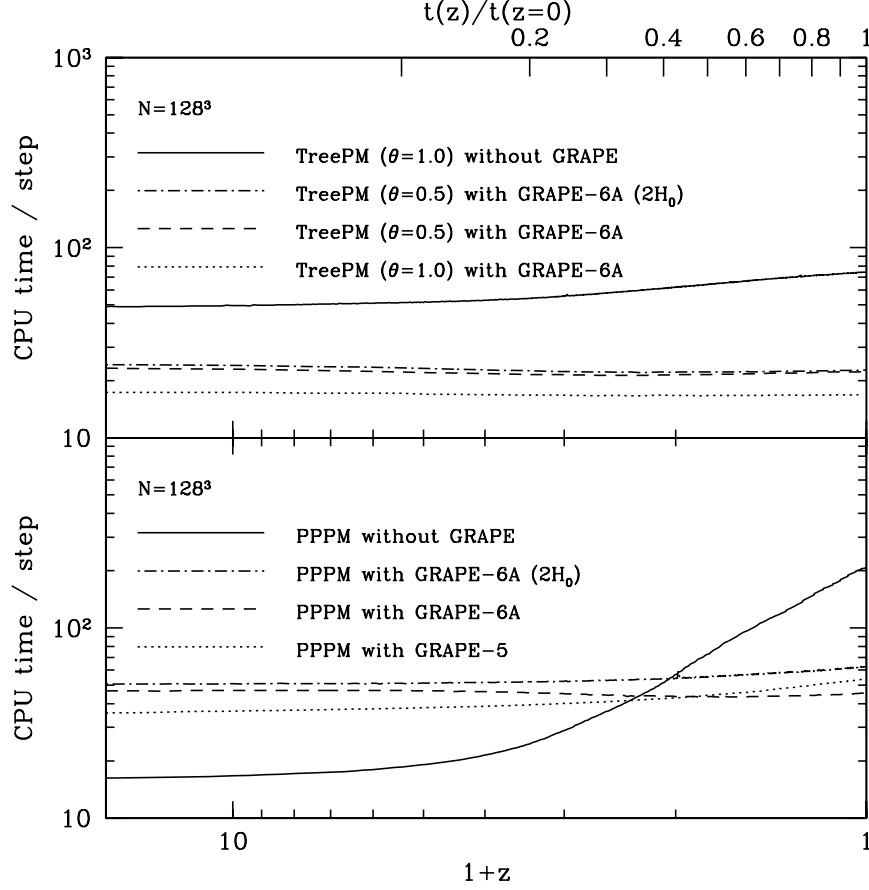


**Fig. 6.** The CPU time per step for the PPPM and TreePM methods. Lines labeled as “2H<sub>0</sub>” indicate the results for the PM grid spacing of twice the standard value.

where  $N_{\text{int}}$ ,  $N$  and  $P$  are the number of interactions and particles, and computational speed of the GRAPE chip, respectively.  $P$  is  $1.28 \times 10^9$  (interactions/sec) and  $2.3 \times 10^9$  (interactions/sec) for GRAPE-5 and GRAPE-6A, respectively. The second term in the parenthesis indicates the pipeline delay in the GRAPE chip. In table 2, the significant differences in the PM calculation time for the runs with and without GRAPE arise from the difference of the adopted PM grid spacing. We can see that the most dominant part is the communication between GRAPE and a host computer, which will be improved in the new versions of GRAPE systems.

### 5.2. Parallel Implementation

Next, we discuss the parallel performance. Figure 8 shows the CPU time (measured with `MPI_wtime()`) for the parallel PPPM (left) and TreePM (right) methods with GRAPE as a function of the number of nodes  $N_p$  for  $N = 128^3$  and  $256^3$ . We could not measure that for  $N_p = 1$  and  $N = 256^3$  owing to a short of memory. The parallel system consists of at maximum 16 nodes each of which consists of one host computer and one GRAPE-6A board. The host computers have Intel Pentium 4 (2.8CGHz, i865G) with 2GB of PC3200 memories for the 1st

**Table 2.** The calculation time with the serial PPPM method for one timestep with GRAPE-5 and GRAPE-6A, and without GRAPE

$N$	$64^3$	$64^3$	$128^3$	$128^3$	$128^3$	$128^3$	$128^3$	$128^3$
redshift	24	24	28	28	28	0	0	0
GRAPE	5	6A	none	5	6A	none	5	6A
PM(sec/step)	0.48	0.4	9.42	4.07	3.43	8.36	4.19	3.38
FFT	0.02	0.02	2.99	0.25	0.21	2.98	0.25	0.22
others	0.46	0.38	6.43	3.82	3.22	5.38	3.94	3.27
PP(sec/step)	4.97	5.42	6.37	30.8	42.5	200	49.5	39.1
GRAPE	0.48	0.25	N/A	1.73	0.90	N/A	11.2	5.81
comm	4.49	5.17	N/A	30.5	41.6	N/A	38.3	33.3
Total(sec/step)	5.43	5.84	16.1	35.3	45.9	210	54.0	42.5

**Table 3.** The calculation time with the serial TreePM method for one timestep with  $\theta = 0.5$  and 1.0

$N$	$64^3$	$64^3$	$128^3$	$128^3$	$128^3$	$128^3$	$128^3$	$128^3$
$\theta$	1.0	0.5	1.0	1.0	0.5	1.0	1.0	0.5
redshift	24	24	28	28	28	0	0	0
GRAPE	6A	6A	none	6A	6A	none	6A	6A
PM(sec/step)	0.41	0.42	8.80	3.86	3.73	8.40	3.75	3.69
FFT	0.02	0.02	2.99	0.20	0.20	2.99	0.20	0.20
others	0.40	0.41	5.81	3.76	3.63	5.41	3.65	3.59
PP(sec/step)	1.58	2.37	39.81	13.13	19.33	66.41	13.07	18.26
tree	0.27	0.47	17.01	2.13	3.62	21.61	2.91	4.68
comm	1.10	1.53	N/A	9.31	12.62	N/A	8.32	10.66
GRAPE	0.21	0.37	N/A	1.69	3.09	N/A	1.84	2.92
Total(sec/step)	2.03	2.83	48.61	17.32	23.39	74.78	16.88	22.28



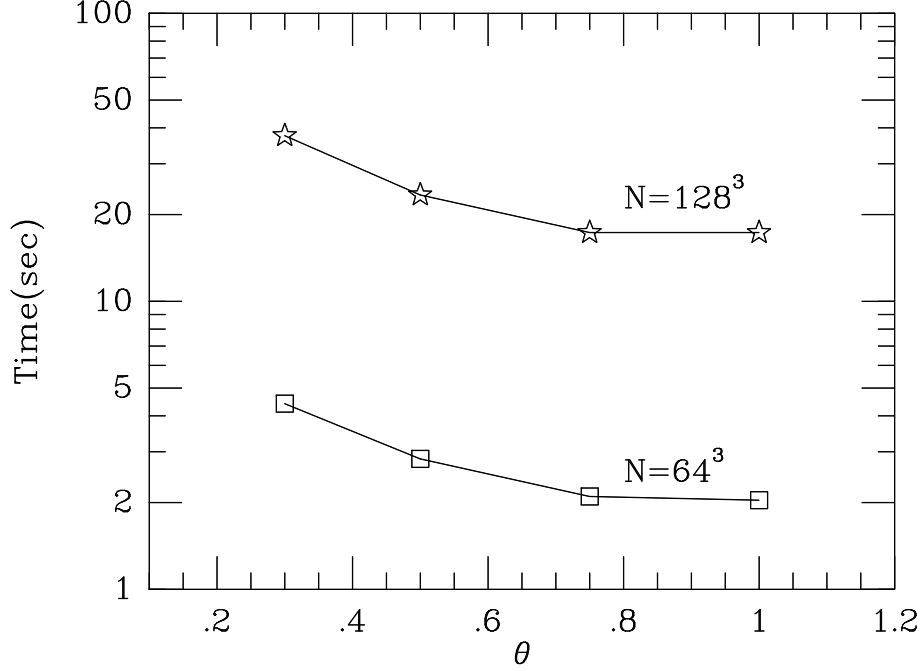


**Fig. 7.** The CPU time per timestep for the TreePM method on GRAPE with single node, as a function of the opening parameter,  $\theta$

to 8th node, and Intel Pentium 4 (2.4BGHz, E7205) with 2GB of PC2100 memories for the 9th to 16th node. We use gcc compiler (version 3.2.2) and MPICH (version 1.2.5.2) on Redhat 9.0. All nodes are connected with Gbit Ethernet via a single switch. We plot the median of those for the first 9 steps from the initial conditions ( $z = 28$  for  $N = 128^3$  and  $z = 39$  for  $N = 256^3$ ).

The right panel of figure 8 shows that our present implementation of the parallel TreePM method obtains moderately good performance up to  $N_p = 8$ . In the case of  $\theta = 1.0$  in which the PP part is less expensive than the  $\theta = 0.5$  case, the parallel scalability is not so good because the time for communication of the PM grid data logarithmically increases as  $N_p$  increases in our present implementation. This can be seen in Table 5, which gives the breakdown of the calculation time per timestep of the 1st node. In the table, "others" include the time for the data exchange and the synchronization. We can see that the scalability is improved in the case of the PM grid spacing,  $2H_0$ . Adopting larger PM grid spacing reduces the communication cost for the PM grid data and the scalability is improved, despite that smaller opening parameter  $\theta$  is required for reasonable force accuracy at initial homogeneous phase as discussed in the previous section. In the parallel PPPM method, the scalability is better than the TreePM method, since the computational cost of PP part is predominant compared with that of the PM part. On the contrary to the parallel TreePM method, larger PM grid spacing does not improve the total performance and the parallel efficiency. As can be seen in Table 4, this is because the larger cutoff radius  $r_{\text{cut}}$  leads to the increase in computational cost required in the PP calculation, despite of the reduction of the communication overhead in the PM part. It

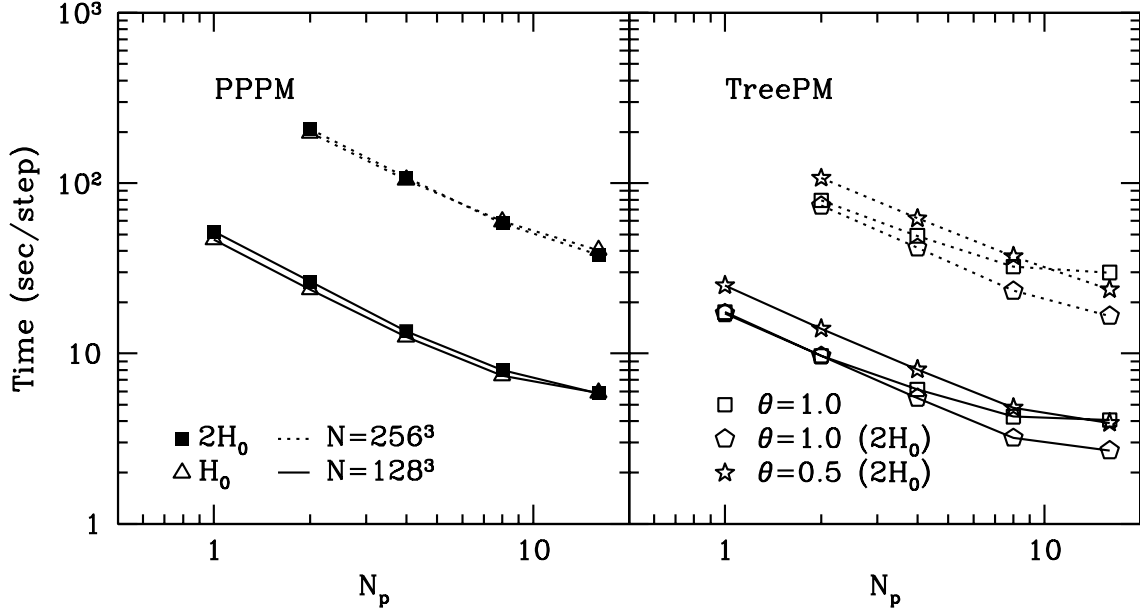


**Fig. 8.** The CPU time per timestep for parallel implementation of the TreePM method on GRAPE as a function of the number of node,  $N_p$ .

must be noted that, for both of the parallel PPPM and TreePM methods, the communication overhead between GRAPE and host computers is dominant time sink, as is also the case with the serial implementations.

In figure 9, we plot the CPU time per timestep as a function of redshift for  $N = 128^3$  and  $N = 256^3$  LCDM simulations using the parallel PPPM and TreePM methods on 16 nodes. Similar to the serial implementations, the CPU time is almost constant irrespective of the redshift or particle clustering. The CPU time in the parallel PPPM method for  $N = 256^3$  slightly increases at  $1 + z \lesssim 1.5$ , and the similar feature can be vaguely seen for the parallel PPPM run with  $N = 128^3$ . This is due to the difference in the number of particles in the skirt regions for each node, which leads to the imbalance of the PP calculation cost among the parallel nodes. In order to prevent this feature, we have to consider more sophisticated schemes for the domain decomposition.

So far, we present the parallel performance for the runs in a relatively large cosmological volume. It is also interesting to measure the parallel performance for very strongly clustered systems, for which it might be expected that the simple one dimensional domain decomposition technique is not so effective. As such an example, we perform parallel runs for the initial condition of the Santa Barbara Cluster Comparison Project (Frenk et al. 1999), which is a constrained initial condition and is set up so that a very massive dark halo with  $\simeq 10^{15} M_\odot$  is eventually formed at  $z = 0$ . In the initial condition, Einstein de-Sitter CDM cosmology with  $\Omega_0 = 1$ ,  $\Omega_\Lambda = 0$ ,  $h = 0.5$  and  $\sigma_8 = 0.9$  is assumed and the size of the simulation volume is set to  $L = 64h^{-1}\text{Mpc}$ . Figure 10 shows the CPU time per step for the parallel runs with 8 PC-

**Table 4.** Breakdown of the calculation time per timestep for the parallel PPPM method on GRAPE-6A.

$N$	$128^3$	$128^3$	$128^3$	$128^3$	$256^3$	$256^3$	$256^3$	$256^3$
PM grid spacing	$H_0$	$H_0$	$2H_0$	$2H_0$	$H_0$	$H_0$	$2H_0$	$2H_0$
$N_p$	2	8	2	8	2	8	2	8
PM (sec/step)	2.26	1.78	1.41	0.49	22.36	14.31	12.60	4.25
internode comm	0.31	0.95	0.08	0.11	2.26	7.20	0.31	0.91
FFT	0.20	0.21	0.02	0.02	2.64	2.71	0.21	0.20
others	1.75	0.62	1.31	0.36	17.46	4.40	12.08	3.14
PP (sec/step)	21.40	5.27	24.94	7.23	174.32	44.04	194.85	53.82
internode comm	0.11	0.12	0.18	0.31	0.41	0.39	0.81	0.89
comm	20.8	5.03	21.48	5.99	170.80	42.86	171.43	46.54
GRAPE	0.46	0.12	3.28	0.93	3.11	0.79	22.61	6.19
others (sec/step)	0.15	0.26	0.27	0.26	0.83	1.08	0.73	0.81
Total (sec/step)	23.81	7.31	26.62	7.98	197.51	59.43	208.18	58.88

**Table 5.** Same as Table 4, but for the parallel TreePM method.

$N$	$128^3$	$128^3$	$128^3$	$128^3$	$128^3$	$128^3$	$256^3$	$256^3$	$256^3$	$256^3$	$256^3$	$256^3$
$\theta$	1.0	1.0	1.0	1.0	0.5	0.5	1.0	1.0	1.0	1.0	0.5	0.5
PM grid spacing	$H_0$	$H_0$	$2H_0$	$2H_0$	$2H_0$	$2H_0$	$H_0$	$H_0$	$2H_0$	$2H_0$	$2H_0$	$2H_0$
$N_p$	2	8	2	8	2	8	2	8	2	8	2	8
PM(sec/step)	2.35	1.58	1.53	0.52	1.49	0.53	22.26	14.35	13.07	4.28	13.07	4.32
internode comm	0.33	0.89	0.07	0.13	0.04	0.14	2.40	7.12	0.32	0.89	0.32	0.94
FFT	0.20	0.20	0.02	0.02	0.02	0.02	2.64	2.74	0.20	0.20	0.20	0.20
others	1.82	0.49	1.44	0.37	1.43	0.37	17.22	4.49	12.55	3.19	12.55	3.18
PP(sec/step)	7.08	2.45	7.90	2.57	12.18	4.19	54.95	16.83	58.63	17.65	92.06	31.87
internode comm	0.11	0.43	0.17	0.38	0.17	0.60	0.72	2.54	0.91	2.64	0.95	2.27
tree	1.17	0.44	1.25	0.39	2.11	1.02	7.57	3.06	10.49	3.11	18.09	4.96
comm	4.96	1.36	5.53	1.56	8.13	2.12	39.82	9.50	39.48	9.95	58.55	20.98
GRAPE	0.84	0.22	0.95	0.24	1.77	0.45	6.84	1.73	7.75	1.95	14.47	3.66
others(sec/step)	0.25	0.23	0.24	0.10	0.30	0.30	1.93	1.16	2.00	1.40	1.95	0.97
Total(sec/step)	9.68	4.26	9.67	3.19	13.97	4.79	79.14	32.34	73.71	23.33	107.08	37.11

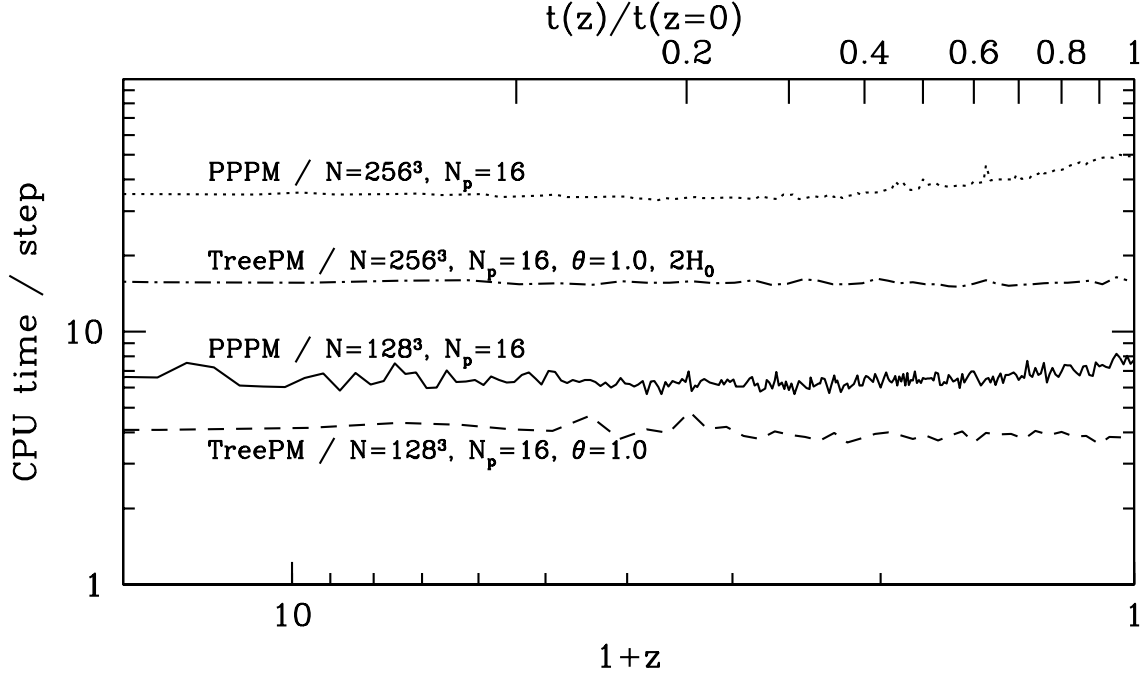


**Fig. 9.** The CPU time per step for the parallel PPPM and TreePM runs with 16 nodes. The upper horizontal axis shows the cosmic time normalized to  $z = 0$ . Lines labeled as “ $2H_0$ ” indicate the results for the PM grid spacing of twice the standard value.

GRAPE nodes for both of the parallel PPPM and TreePM implementations. In the parallel TreePM implementation, we adopt the opening parameter of  $\theta = 1.0$  and the PM grid spacing of  $H = 2H_0$ . In the parallel TreePM run, the CPU time per step is almost constant and the simple one dimensional domain decomposition works well even under the strong clustering at lower redshift. On the other hand, in the parallel PPPM run, significant increase of CPU time per step can be seen at lower redshift  $1+z \lesssim 1.5$ , which is again caused by the imbalance of number of particles in the skirt regions. Since, at lower redshift, we have strongly clustered particles as a very massive dark halo, such an imbalance of number of particles in the skirt regions is more serious than that for unconstrained runs shown in figure 9.

## 6. Memory Consumption

In the PPPM implementation, the memory consumption can be approximately estimated as

$$112 \left( \frac{N}{128^3} \right) + 9 \left( \frac{N_{\text{PM}}}{128} \right)^3 \text{ Mbytes}, \quad (8)$$

where  $N$  is the number of particles,  $N_{\text{PM}}$  the number of PM grid per side. The first term is for the data of particles and the linked-list structure, and the second one is for the PM grid and the data for the Green’s function used in the PM calculation. Note that, for the run with the number of particles of  $N$  on GRAPE, we usually adopt  $N_{\text{PM}} = N^{1/3}$  as an optimal value

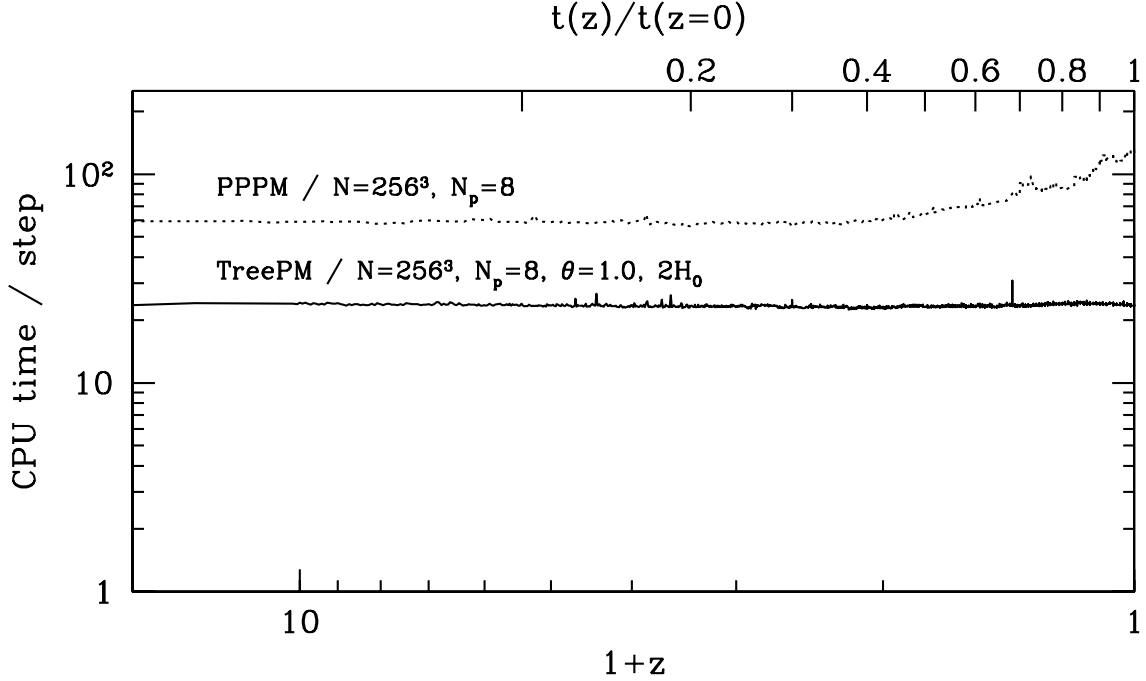


**Fig. 10.** The CPU time per step for the parallel runs for the initial condition of the Santa Barbara Cluster Comparison Project.

for the efficient use of GRAPE. In the TreePM implementation, the memory requirement is approximately estimated as

$$104 \left( \frac{N}{128^3} \right) + 60 \left( \frac{N}{128^3} \right) + 9 \left( \frac{N_{\text{PM}}}{128} \right)^3 \text{ Mbytes}, \quad (9)$$

where the first, second and third terms are for particles, tree structure and PM grid data, respectively.  $N_{\text{PM}}$  is set to  $N_{\text{PM}} = N^{1/3}$  as the PPPM implementation just for the efficient use of GRAPE. The factor 60 for tree structure is rather small compare to usual implementations of the tree algorithm. This is because we allow leaf nodes to have more than one particle, and stop the subdivision of tree node if the number of particles belonging the node is less than 30, up to which the calculation cost does not increase so much. The memory consumption of our PPPM implementation considerably less than that of the TreePM method since the tree structure requires significant amount of memory, though the memory consumption for the chaining cells used in the PPPM method is negligible compared with the total memory consumption.

In the parallel implementation, each node is responsible for roughly  $N/N_p$  particles and requires an extra memory for the communication with the neighboring nodes. In the parallel PPPM and TreePM method, the extra memory is used for the imported particles in the skirt regions as depicted in figure 2, and for the interaction list of the neighboring nodes, respectively. Thus, for the parallel PPPM method, the memory consumption in each node is approximately expressed by replacing the number of particles  $N$  in equation (8) with  $N/N_p + 2N/N_{\text{cc}}$ . The second term roughly indicates the number of particles in the skirt regions.

Here,  $N_{\text{cc}}$  is the number of chaining cells per side and is usually set to  $N_{\text{cc}} \simeq L/r_{\text{cut}} = N^{1/3}/3$  in our implementation. For the parallel TreePM method, we can approximate the memory consumption for each node by replacing  $N$  in equation (7) by  $N/N_p + \beta$ . The second term,  $\beta$ , indicates the number of interaction lists imported from the neighboring domains. It depends on the opening parameter,  $\theta$ , and its dependences on  $N$  and  $N_p$  are very weak. In the case of  $N = 256^3$ ,  $\theta = 1.0$  and  $N_p = 8$ ,  $\beta \sim 5 \times 10^5$ .

## 7. Conclusion and Discussion

In this paper, we present the PPPM and TreePM implementation of cosmological N-body simulations on GRAPE-5 and GRAPE-6A for both of a single processor and parallel systems. The most remarkable feature of our implementations is that the CPU time per timestep is almost constant irrespective of the clustering degree of the particles. As for the PPPM method, the use of GRAPE overcomes its main disadvantage in which PP calculation cost significantly increases as particle clustering develops. Under strong particle clustering, our PPPM implementation with GRAPE-5 and -6A is 4–5 times faster than that without GRAPE, and sufficiently fast even compared with the PPPM implementation on MDGRAPE-2 shown in Susukita (2004). In comparison between the PPPM and TreePM implementations on GRAPE, the TreePM method has better performance (i.e. shorter CPU time), although the PPPM method has advantage in its memory consumption and force accuracy. The CPU time per timestep in the TreePM method with opening parameter  $\theta = 1.0$  is less than half of that in the PPPM method.

Since smaller opening parameter gives better force accuracy but poorer performance, trade-off between force accuracy and performance has to be made in the TreePM method. According to figures 3 and 4, the force accuracy for  $\theta = 1.0$  is as good as that of the PPPM method when the standard PM grid spacing of  $H_0$  is adopted. On the other hand, in the case of the PM grid spacing of  $2H_0$ , the force accuracy is degraded under the nearly homogeneous particle distribution, and thus, we have to reduce  $\theta$  to  $\simeq 0.5$  in order to reproduce the same level of force accuracy as for the standard PM grid spacing. Therefore, the most optimal set of  $\theta$  and  $H$  is  $\theta = 1.0$  and  $H = H_0$  or  $\theta = 0.5$  and  $H = 2H_0$ . The combination of  $\theta = 1.0$  and  $H = 2H_0$  is acceptable only for the situation where the particle clustering is strong enough (for example,  $z < 4$  in the LCDM simulation with  $N = 128^3$  particles as shown in figure 4). In parallel runs, as described in § 5, adopting larger PM grid spacing significantly contributes to reduce the communication among the parallel nodes.

Further improvement of GRAPE system with up-to-date technology would provide more powerful computing systems for the PPPM and TreePM methods. As is clear in the breakdown in Table 2 and 3, the total performance is limited by the communication speed between the host computer and GRAPE. For the communication, GRAPE-5 and 6A uses rather old technology (PCI interface 32bit/33MHz). We are currently developing new versions of GRAPE system (GRAPE-7 and GRAPE-DR) which adopt new interface technology, such as PCI-X and PCI

Express. Using this new interface technology, together with a new GRAPE processor chip, 3-10 times speedup for single node performance is expected to be obtained.

We are grateful to Takayuki Saitoh, Atsushi Kawai, Junichiro Makino and Naoto Miyazaki for their technical advices and helpful discussions. We also thank an anonymous referee for useful comments and suggestions. KY acknowledge support from the Japan Society for the Promotion of Science. This research was supported in part by the Grants-in-Aid by Japan Society for the Promotion of Science (14740127, 15·10351) and by the Ministry of Education, Science, Sports, and Culture of Japan (16684002).

## References

- Bagla, J.S. 2002, *J. Astrophys. Astr.*, 23, 185  
Barnes, J.E., & Hut, P. 1986, *Nature*, 324, 446  
Barnes, J.E. 1990, *J. Comp. Phys.*, 87, 161  
Bertschinger, E. & Gelb, J. 1991, *Comp. Phys.*, 5, 164  
Bode, P., Ostriker, J.P., Xu, G. 2000, *ApJS*, 128, 561  
Bode, P., & Ostriker, J.P. 2003, *ApJS*, 145, 1  
Briau, P.P., Summers, F.J., Ostriker, J.P. 1995, *ApJ*, 453, 566  
Briau, P.P., & Evrard, A.E. 2000, *New Astron.*, 5, 163  
Couchman, H.M.P. 1991, *ApJ*, 368, L23  
Dubinski, J. Kim, J., Park, C., Humble, R. 2003, *New Astron.*, 9, 111  
Eastwood, J.W., Hockney, R.W., & Lawrence, D.N., 1980, *Comput. Phys. Commun.* 1980, 19, 215  
Efstathiou, G., & Eastwood, J.W. 1981, *MNRAS*, 194, 503  
Efstathiou, G., Davis, M., Frenk, C.S., & White, S.D.M. 1985, *ApJS*, 57, 241  
Frenk, C.S. et al. 1999, *ApJ*, 525, 554  
Fukushige, T., Taiji, M., Makino, J., Ebisuzaki, T., & Sugimoto, D. 1996, *ApJ*, 468, 51  
Fukushige, T. & Suto, Y. 2001, *ApJ*, 557, L11  
Fukushige, T., Makino, J., & Kawai, A. 2005, submitted to *PASJ*  
Hockney, R.W., & Eastwood, J.W. 1981, *Computer Simulation Using Particles* (New York:McGraw-Hill)  
Jing, Y.P. & Fang, L. 1994, *ApJ*, 432, 438  
Jing, Y.P. & Suto, Y. 1998, *ApJL*, 494, L5  
Kawai, A., Fukushige, T., Makino, J., & Taiji, M. 2000, *PASJ*, 52, 659  
Makino, J. 1991, *PASJ*, 43, 621  
Makino, J., & Taiji, M. 1998, *Scientific Simulations with Special Purpose Computers — The GRAPE Systems* (John Wiley and Sons, Chichester)  
Makino, J., Fukushige, T., Koga, M., & Namura, K. 2003, *PASJ*, 55, 1163  
Okumura, S.K., Makino, J., Ebisuzaki, T., Fukushige, T., Ito, T., Sugimoto, D., Hashimoto, E., Tomida, K., Miyakawa, N., 1993, *PASJ*, 45, 329  
Susukita, R. 2004, *ApJS*, 153, 1



- Susukita, R., et al. 2003, *Comput. Phys. Commun.*, 155, 115
- Sugimoto, D., Chikada, Y., Makino, J., Ito, T., Ebisuzaki, T., & Umemura, M. 1990, *Nature*, 345, 33
- Thomas, P. & Couchman H.M.P., 1992, *MNRAS*, 257, 11
- Yoshikawa, K., Jing, Y.P., & Suto, Y. 2001, *ApJ*, 535, 593
- Yoshikawa, K., Taruya, A., Jing, Y.P., & Suto, Y. 2001, *ApJ*, 558, 520
- Xu, G. 1995, *ApJS*, 98, 355